JOC*Article*

Tautomeric Equilibria of [1]Benzopyrano[3,4-*d*]imidazol-4(3*H*)-ones, a Theoretical and NMR Study

Alessandro Contini,* Donatella Nava, and Pasqualina Trimarco

Istituto di Chimica Organica "Alessandro Marchesini", Facoltà di Farmacia, Università degli Studi di Milano, Via Venezian 21, 20133 Milano, Italy

alessandro.contini@unimi.it

Received September 14, 2005

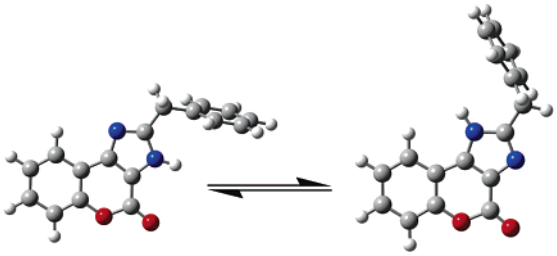

Benzopyranoimidazolones could virtually exist in four tautomeric forms, namely N3−H, N1−H, coumarin O−H, and C2−H. Experimental evidence reported thus far has been unable to lead to a unique statement about the preferred tautomeric forms in solution. In this work, tautomeric equilibria for a series of 2-substituted [1]benzopyrano[3,4-*d*]imidazol-4(3*H*)-ones were investigated by DFT calculations, in both gas phase and solution. The influence of the solvent was included in the calculations by the CPCM solvent model. ^{13}C chemical shifts of all tautomers were computed at different levels of theory and then compared with experiments to assign the preferred tautomers. Theoretical findings were then compared to dynamic ^{1}H NMR experiments results.

Introduction

The development of novel synthetic strategies for achieving compounds containing the coumarin nucleus condensed to several heterocycles has been the subject of our research for the past few years.[1−3] Such heterocycles are pharmacologically relevant as CNS depressants,[4] growth inhibitors of mammalian cancer,[5] and also phosphodiesterase VII inhibitors for treatment of immunity-associated diseases.[6] Furthermore, the study and the quantitative evaluation of prototropic tautomerism in heterocyclic compounds are of primary interest, influencing both chemical and biological behavior as, for example, the ability of a drug to bind the active site of a target enzyme.[7] Indeed, as shown in Figure 1, the pyranoimidazolonic moiety could be considered as a conformationally constrained peptidomimetic structure, and this could be reflected in the ability of such heterocycles to interact with biologically important macromolecules.

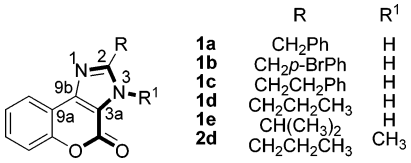

FIGURE 1. [1]Benzopyrano[3,4-*d*]imidazol-4(3*H*)-ones investigated in the present study.

We recently reported the synthesis of substituted benzopyranoimidazolones represented in Figure 1, and we pointed out

* Corresponding author. Phone: +390250314480. Fax: +390250314476.

(1) Beccalli, E. M.; Contini, A.; Trimarco, P. *Tetrahedron* **2005**, *61*, 4957−4964.

(2) Beccalli, E. M.; Contini, A.; Trimarco, P. *Tetrahedron Lett.* **2004**, *45*, 3447−3449.

(3) Beccalli, E. M.; Contini, A.; Trimarco, P. *Eur. J. Org. Chem.* **2003**, 3976−3984.

(4) Savel'ev, V. L.; Pryanishnikova, N. T.; Zagorevskii, V. A.; Chernyakova, I. V.; Artamonova, O. S.; Shavyrina, V. V.; Malysheva, L. I., *Khim.-Farm. Zh.* **1983**, *17*, 697−700.

(5) Trkovnik, M.; Kalaj, V.; Kitan, D. *Org. Prep. Proced. Int.* **1987**, *19*, 450−455.

(6) Eggenweiler, M.; Rochus, J.; Wolf, M.; Gassen, M.; Poeschke, O. Merck Patent Gmbh, Germany, PCT Int. Appl., 2001; *Chem. Abstr.* **2001**, *134*, 331619.

(7) Pospisil, P.; Ballmer, P.; Folkers, G.; Scapozza, L. Tautomerism of nucleobase derivatives and their score in virtual screening to thymidine kinase. *Abstracts of Papers*, 224th National Meeting of the American Chemical Society, Boston, MA, Aug 18−22, 2002; American Chemical Society: Washington, DC, 2002.

10.1021/jo0519256 CCC: $33.50
Published on Web 12/01/2005

SCHEME 1. Tautomeric Equilibria for Compounds 1a−e

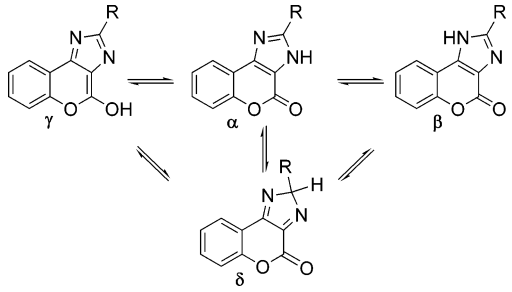

the possibility for compounds **1a**−**e** to exist in solution in at least two tautomeric forms, the N3−H and the N1−H tautomers.[3] However, as depicted in Scheme 1, coumarin condensed imidazoles could exist in four probable tautomeric forms, namely N3−H (α tautomer), N1−H (*β* tautomer), coumarin O−H (*γ* tautomer), and C2−H (*δ* tautomer). The *γ* tautomer was ruled out because the IR spectra of all the benzopyranoimidazolones **1a**−**e**, recorded in chloroform solution, exhibited only the typical lactone bands at 1704−1712 cm^{-1}, whereas the OH stretching at 3000−3500 cm^{-1} was never detected. The *δ* form was never observed by us on the basis of ^1H and ^{13}C NMR spectra; however, C−H forms were reported as possible tautomers for substituted imidazoles.[8] Moreover, experiments previously reported in the literature were unable to unequivocally assign the preferred tautomeric structure,[3] and in two independent articles opposite tautomeric structures were assigned to the same compound.[5,9] An attempt to determine the preferred tautomeric structure was done through the N-methylation of compound **1d**, where only the N3−CH_3 product **2d** was isolated at both high and low reaction temperatures.[3] This result led to the conclusion that **1d** α tautomer is the most reactive toward methylation in the adopted reaction conditions; however, no statements could be made about the relative stability if such tautomers show a fast equilibrium in solution. On the other hand, tautomerism was successfully described for various substituted imidazoles by ab initio and DFT calculations in both gas phase and solution within the continuum solvent model or evaluating explicit solvent interactions.[10−15]

In our previous work, where the main objective was the development of a synthetic strategy for benzopyranoimidazolones, preliminary quantum chemical calculations explained only in part the tautomeric behavior observed, and thus the need for a thorough theoretical and experimental investigation. In the study reported here, with the aim to clarify the tautomeric equilibrium of benzopyranoimidazolones, the relative stability of the possible tautomers for **1a**−**e** was evaluated by mean of B3LYP calculations, including the solvent contribution by the SCRF CPCM model. Furthermore, the ^{13}C chemical shifts were calculated for α and *β* tautomers by GIAO technique at the B3LYP/TZVP levels of theory and compared to the experiments. The comparison of theoretically computed and experimental chemical shifts was reported as a reliable method for the structural determination of organic compounds[15] as well as for the investigation of tautomeric equilibrium of heterocyclic compounds.[16−20] Moreover, dynamic ^1H NMR spectra were recorded in acetone at a temperature range from room temperature to 173 K to evidence and quantify all possible tautomers in solution by lowering their conversion rate.

TABLE 1. Relative Enthalpies[a] (kcal/mol) Calculated in Gas Phase, in DMSO, and in Acetone[b] for α, *β*, *γ*, and *δ* Tautomers of Compounds 1a−e, Together with Dipole Moments *μ* (in Debyes) and Percent Population

		Δ*H*				*μ*[c]		population[d]	
entry	solvent	α	*β*	*γ*	*δ*	α	*β*	α%	*β*%
1a	gas phase	0.0	4.4	23.1	30.9	3.68	8.39	99.9	0.1
	DMSO	0.0	0.7	22.6	30.8	4.34	12.05	77.0	23.0
	acetone	0.0	0.9	22.5	30.9	4.31	11.92	81.0	19.0
1b	gas phase	0.0	4.3	22.0	30.2	3.62	6.95	99.9	0.1
	DMSO	0.0	0.7	22.7	31.4	4.80	10.31	76.3	23.7
	acetone	0.0	0.8	22.6	31.5	4.74	10.19	78.4	21.6
1c	gas phase	0.0	4.0	22.2	32.2	3.70	8.61	99.9	0.1
	DMSO	0.0	1.3	21.4	32.2	4.54	11.94	90.2	9.8
	acetone	0.0	1.4	21.2	32.3	4.50	11.81	91.5	8.5
1d	gas phase	0.0	4.7	21.7	30.7	3.72	8.18	100.0	0.0
	DMSO	0.0	0.2	23.9	34.2	4.47	12.28	57.0	39.1
	acetone	0.0	0.3	23.8	34.0	4.44	12.13	60.9	33.5
1e	gas phase	0.0	4.9	21.8	30.4	3.66	7.97	100.0	0.0
	DMSO	0.0	0.1	24.2	33.4	4.48	12.18	56.0	44.0
	acetone	0.0	0.4	24.1	33.3	4.45	12.01	66.5	33.4

[a] The enthalpy of the most stable tautomer for each entry is taken as reference. [b] Calculated from the sum of B3LYP/TZVP energy and the thermal correction to enthalpy obtained from thermochemical calculations (298.15 K, 1 atm) at the B3LYP/6-31G** level. [c] Calculated at the B3LYP/TZVP//B3LYP/6-31G** level. [d] Calculated accordingly to the Boltzmann's equation at $T = 298$ K.

Results and Discussion

Despite experimental evidence, in our opinion an exhaustive theoretical study on tautomerism of benzopyranoimidazolones should include all the potential tautomeric forms depicted in Scheme 1. Moreover, the comparison of the energies of experimentally observed and theoretical tautomers could be an effective strategy to evaluate the reliability of the chosen computational methods. The values of the relative enthalpies (kcal/mol) of all the tautomeric forms of compounds **1a**−**e** are reported in Table 1. As expected, the first evidence from both vacuum and solution calculations, performed with the CPCM solvent model for DMSO and acetone, was that the α and the *β* forms are the only relevant tautomers of benzopyranoimidazolones. Indeed, gas phase and solution relative energies of the *γ* and *δ* tautomers resulted from 21.2 to 24.2 and from 30.2 to 34.2 kcal/mol, respectively, higher if compared with the most favored α form. The probability of observing either the O−H or the C−H form both in gas phase and in solution is thus minimal, confirming the previously reported experimental

(8) Abou-Jneid, R.; Ghoulami, S.; Martin, M. T.; Tran Huu Dau, E.; Travert, N.; Al-Mourabit, A. *Org. Lett.* **2004**, *6*, 3933−3936.
(9) Tabakoviæ, K.; Tabaković, I. *Croat. Chem. Acta* **1981**, *54*, 451−458.
(10) Worth, G. A.; King, P. M.; Richards, W. G. *Biochim. Biophys. Acta* **1989**, *993*, 134−136.
(11) Li, G.-S.; Ruiz-Lopez, M. F.; Zhang, M.-S.; Maigret, B. *J. Mol. Struct.: THEOCHEM* **1998**, *422*, 197−204.
(12) Shishkin, O. V.; Sukhanov, O. S.; Gorb, L.; Leszczynski, J. *Phys. Chem. Chem. Phys.* **2002**, *4*, 5359−5364.
(13) Raczyńska, E. D. *Anal. Chim. Acta* **1997**, *348*, 431−441.
(14) Li, G.-S.; Ruiz-Lopez, M. F.; Zhang, M.-S.; Maigret, B. *J. Phys. Chem.* **1997**, *101*, 7885−7892.
(15) Claramunt, R. M.; Santa Maria, M. D.; Infantes, L.; Cano, F. H.; Elguero, J. *J. Chem. Soc., Perkin Trans. 2* **2002**, *2*, 564−568.
(16) Luque, F. J.; Lopez-Bes, J. M.; Cemeli, J.; Aroztegui, M.; Orozco, M. *Theor. Chem. Acc.* **1997**, *96*, 105−113.
(17) Claramunt, R. M.; García, M. Á.; López, C.; Trofimenko, S.; Yap, G. P. A.; Alkorta, I.; Elguero, J. *Magn. Reson. Chem.* **2005**, *43*, 89−91.
(18) Alkorta, I.; Elguero, J. *Struct. Chem.* **2003**, *14*, 377−389.
(19) Kleinpeter, E.; Koch, A. *J. Phys. Org. Chem.* **2001**, *14*, 566−576.
(20) Mazurek, A. P.; Dobrowolski, J. Cz.; Sadlej, J. *J. Mol. Struct.* **1997**, *436*−*437*, 435−441.

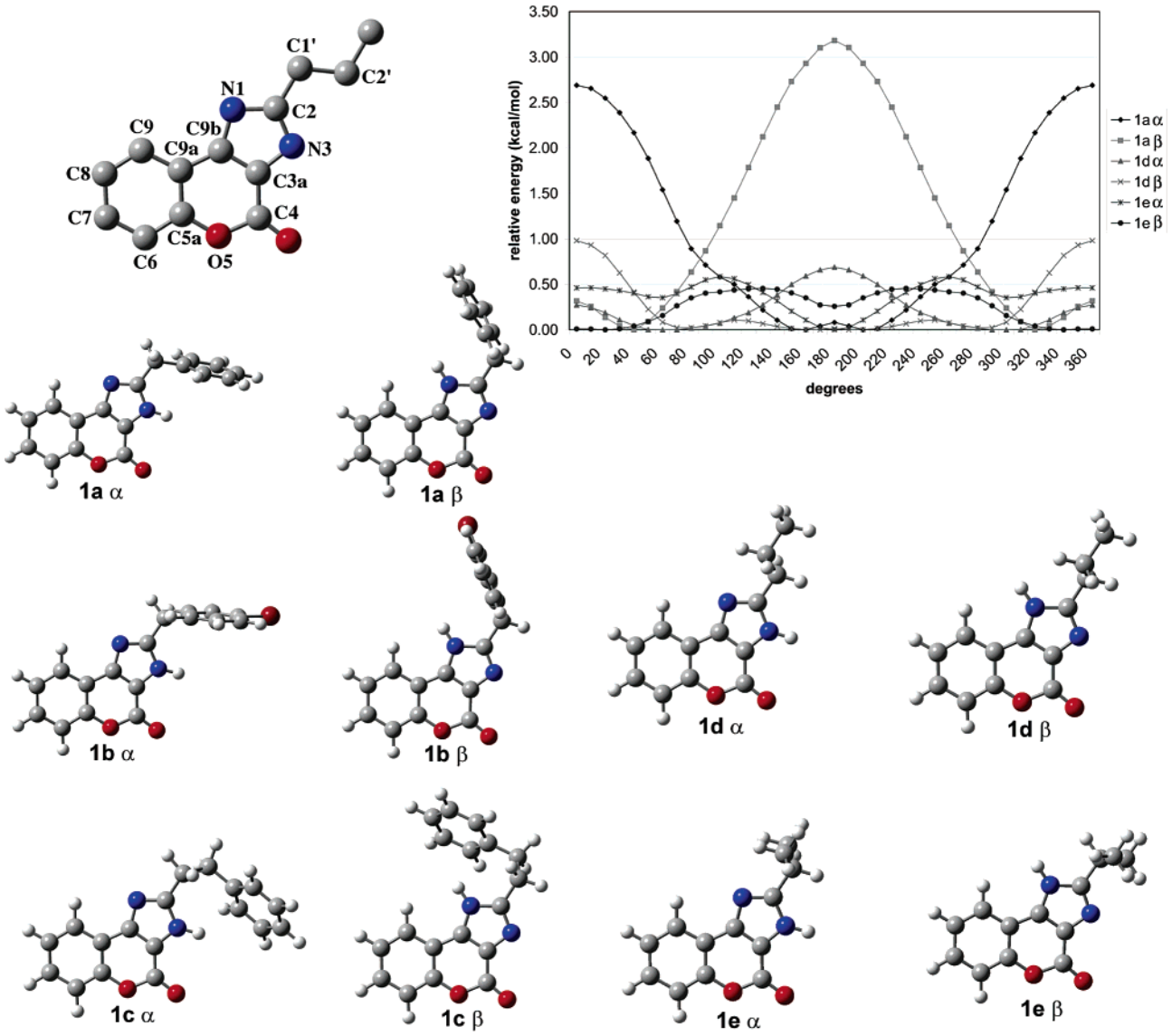

FIGURE 2. Potential energy surface scan of the N1−C2−C1′−C2′ and N1−C2−C1′−H dihedrals for compounds **1a**,**d** and **1e**, respectively, together with minimum energy conformers for the α and *β* tautomers of **1a**−**e**.

observations. Concerning the two N−H tautomers, the vacuum preferred form is decidedly the α tautomer, which was more stable than *β* from 4.0 to 4.9 kcal/mol, as observed for compounds **1c** and **1e**, respectively. Thus, according to Boltzmann's equation, the calculated population of the α tautomer in the gas phase and in standard conditions resulted in more than 99% for all the investigated compounds. The introduction of the solvent contribution gave rise to a drop of the *β*−α energy difference, and relative enthalpies resulted between 0.1 and 1.3 kcal/mol in DMSO as observed for **1e** and **1c**, respectively, and from 0.2 to 1.4 in acetone, as observed for **1d** and **1c**, respectively.

Energy values reported in Table 1 show that the solvent acted by stabilizing the *β* relative to the α tautomer, while on the *γ* and *δ* forms it had almost no effect for compounds **1a**−**c** and it even destabilized the latter tautomers for compounds **1d**,**e**. The major relative stabilization of the *β* tautomer in polar solvents, such as DMSO and acetone, is not surprising taking into account its higher dipole moment and thus its higher affinity for the polar solvation medium. As expected, the effect of DMSO on the *β* tautomer stabilization was slightly more evident, although differences among the two solvents were not particularly relevant.

Concerning geometrical features, we noted that the C2 substituent oriented differently in the two tautomeric forms. As depicted in Figure 2, in the case of **1a**−**c** the aromatic moiety pointed always toward the tautomeric hydrogen, and in our opinion, such conformation is stabilized by a N−H···Ar weak hydrogen bond and by a C−H···N interaction between the side-chain aliphatic hydrogens and the sp^2 nitrogen. For compounds **1d**,**e**, on the other hand, the lowest energy conformers could be stabilized by only this latter interaction, and a lower rotational barrier would be expected in those latter cases. Indeed, the ability of a carbon atom, even aliphatic, to act as a donor as well as the possibility for an aromatic ring to act as an acceptor in weak hydrogen bonds are well-known,[35,36] and reported in the literature are several examples of the role of such interactions in influencing the geometrical conformation of molecules in both solution and solid state.[37−39] Donor−acceptor parameters measured for the most stable conformers of compounds **1a**−**e** and summarized in Table 2 are comparable with values reported in the literature.[37−40]

TABLE 2. Weak Hydrogen Interactions Distances and Angles of 1a−e

		distances (Å)				angles (deg)	
entry		HN···Ph[a]	HC···N	NH···Ph	CH···N	N−H···Ph	C−H···N
1a	α	3.81	2.51	3.25	2.66	116.3	70.2
	β	3.88	2.51	3.38	2.62	112.6	72.3
1b	α	3.89	2.51	3.40	2.62	111.1	72.3
	β	3.97	2.51	3.55	2.59	107.4	73.4
1c[b]	α	3.81	2.50	2.98	2.55	139.8	75.1
	β	3.72	2.50	2.88	2.56	141.3	74.4
		HC1′···N	HC2′···N	C1′H···N	C2′H···N	C1′−H···N	C2′−H···N
1d	α	2.51	3.10	2.86	2.79	60.72	95.9
	β	2.50	3.50	2.60	3.37	72.8	87.8
1e	α	2.51	3.11	3.36	2.86	33.1	92.4
	β	2.51	2.99	3.34	2.74	34.7	92.2

[a] The aromatic ring centroid was considered as the acceptor. [b] In this case, a 2D potential energy surface scan at the DFT level was unfeasible in terms of CPU time, while semiempirical calculations conducted on compounds **1a**−**e** provided unreliable results.

Interestingly, compounds **1d** α and **1e** α,β provided the most evident weak hydrogen interaction between the sp^2 nitrogen and the C2′ linked hydrogen, while for **1d** β the main H-bond donor resulted in C1′. Seeking further confirmation, we performed a potential energy surface scan for the rotation of the C2−C1′ bond for both tautomeric forms of compounds **1a**,**d**,**e**, at the B3LYP/6-31G** level.[41] As one can see from the chart on the top right of Figure 2, rotational barriers for compound **1a** resulted in 2.7 and 3.2 kcal/mol for the α and β tautomer, respectively, while for compound **1d** they were 0.7 and 1.0 kcal/mol for the α and β tautomers, respectively. Compound **1e** showed an even lower barrier, with relative energies of 0.6 and 0.5 kcal/mol for the α and β forms, respectively, confirming a weaker conformational stabilization for the latter compounds and strengthening our hypothesis.

Energy values reported in Table 1 showed that the α−β tautomeric equilibrium is certainly possible for all the investigated compounds. Energetic differences between the α and β tautomers were quite homogeneous among compounds **1a**−**e**, and relative energy differences between α and β are very close to the accuracy limit expected for the computational methods employed. For this reason, it was warranted to validate the previous estimations.

Calculation of the ^{13}C Chemical Shifts of 1a−e. In the case of an equilibrium faster than the NMR time scale, such as that observed for proton exchange,[42] an estimation of the equilibrium position could be made by a comparison of the experimental chemical shifts with those theoretically computed for the single tautomers.[19] For the above reasons, ^{13}C absolute shieldings σ were computed using the GIAO method at the B3LYP/TZVP//B3LYP/6-31G** level for the α and β tautomeric forms of compounds **1a**−**e** and then converted in chemical shifts δ for better correlation with experiments, as described in the Theoretical Calculations section. As depicted in Figure 3 for compound **1a**, the obtained fit between theoretical and experimental values is very good, particularly in the region above 100 ppm where the deviations were generally lower than 1%. Substantially higher deviations were found for those carbons that are strongly influenced by the tautomeric rearrangement, namely C2, C3a, C9, C9a, and C9b, where the experimental value resulted as a weighted average of the chemical shifts of the single tautomers. The relative populations for both tautomers, and thus the position of the equilibrium, were then derived from the quadratic sum of the deviations between the theoretically computed chemical shifts for the single tautomers and the experimental values (Table

(21) Frisch, M. J.; Trucks, G. W.; Schlegel, H. B.; Scuseria, G. E.; Robb, M. A.; Cheeseman, J. R.; Zakrzewski, V. G.; Montgomery, J. A., Jr.; Stratmann, R. E.; Burant, J. C.; Dapprich, S.; Millam, J. M.; Daniels, A. D.; Kudin, K. N.; Strain, M. C.; Farkas, O.; Tomasi, J.; Barone, V.; Cossi, M.; Cammi, R.; Mennucci, B.; Pomelli, C.; Adamo, C.; Clifford, S.; Ochterski, J.; Petersson, G. A.; Ayala, P. Y.; Cui, Q.; Morokuma, K.; Malick, D. K.; Rabuck, A. D.; Raghavachari, K.; Foresman, J. B.; Cioslowski, J.; Ortiz, J. V.; Stefanov, B. B.; Liu, G.; Liashenko, A.; Piskorz, P.; Komaromi, I.; Gomperts, R.; Martin, R. L.; Fox, D. J.; Keith, T.; Al-Laham, M. A.; Peng, C. Y.; Nanayakkara, A.; Gonzalez, C.; Challacombe, M.; Gill, P. M. W.; Johnson, B. G.; Chen, W.; Wong, M. W.; Andres, J. L.; Head-Gordon, M.; Replogle, E. S.; Pople, J. A. *Gaussian 98*, revision A.7; Gaussian, Inc.: Pittsburgh, PA, 1998.

(22) Frisch, M. J.; Trucks, G. W.; Schlegel, H. B.; Scuseria, G. E.; Robb, M. A.; Cheeseman, J. R.; Montgomery, J. A., Jr.; Vreven, T.; Kudin, K. N.; Burant, J. C.; Millam, J. M.; Iyengar, S. S.; Tomasi, J.; Barone, V.; Mennucci, B.; Cossi, M.; Scalmani, G.; Rega, N.; Petersson, G. A.; Nakatsuji, H.; Hada, M.; Ehara, M.; Toyota, K.; Fukuda, R.; Hasegawa, J.; Ishida, M.; Nakajima, T.; Honda, Y.; Kitao, O.; Nakai, H.; Klene, M.; Li, X.; Knox, J. E.; Hratchian, H. P.; Cross, J. B.; Bakken, V.; Adamo, C.; Jaramillo, J.; Gomperts, R.; Stratmann, R. E.; Yazyev, O.; Austin, A. J.; Cammi, R.; Pomelli, C.; Ochterski, J. W.; Ayala, P. Y.; Morokuma, K.; Voth, G. A.; Salvador, P.; Dannenberg, J. J.; Zakrzewski, V. G.; Dapprich, S.; Daniels, A. D.; Strain, M. C.; Farkas, O.; Malick, D. K.; Rabuck, A. D.; Raghavachari, K.; Foresman, J. B.; Ortiz, J. V.; Cui, Q.; Baboul, A. G.; Clifford, S.; Cioslowski, J.; Stefanov, B. B.; Liu, G.; Liashenko, A.; Piskorz, P.; Komaromi, I.; Martin, R. L.; Fox, D. J.; Keith, T.; Al-Laham, M. A.; Peng, C. Y.; Nanayakkara, A.; Challacombe, M.; Gill, P. M. W.; Johnson, B.; Chen, W.; Wong, M. W.; Gonzalez, C.; Pople, J. A. *Gaussian 03*, revision B.04; Gaussian, Inc.: Wallingford, CT, 2004.

(23) Dewar, M. J. S.; Zoebisch, E. G.; Healy, E. F.; Stewart, J. J. P. *J. Am. Chem. Soc.* **1985**, *107*, 3902−3909.

(24) Becke, A. D. *J. Chem. Phys.* **1993**, *98*, 5648−5652.

(25) Frisch, M. J.; Pople, J. A.; Binkley, J. S. *J. Chem. Phys.* **1984**, *80*, 3265−3269.

(26) Cammi, R.; Mennucci, B.; Tomasi, J. *J. Phys. Chem. A* **2000**, *104*, 5631−5637.

(27) Eckert, F.; Klamt, A. *AIChE J.* **2002**, *48*, 369−385.

(28) Schaefer, A.; Huber, C.; Ahlrichs, R. *J. Chem. Phys.* **1994**, *100*, 5829−5835.

(29) Ditchfield, R. *J. Chem. Phys.* **1972**, *56*, 5688−5691.

(30) Wolinski, K.; Hinton, J. F.; Pulay, P. *J. Am. Chem. Soc.* **1990**, *112*, 8251−8260.

(31) Davidson, E. R. *Chem. Phys. Lett.* **1996**, *260*, 514−518.

(32) Ośmialowski, B.; Kolehmainen, E.; Gawinecki, R. *Magn. Reson. Chem.* **2001**, *39*, 334−340.

(33) Kutzelnnig, W.; Fleischer, U.; Schindler, M. In *NMR Basic Principles and Progress*; Diehl, P., Fluck, E., Gunther, H., Kosfeld, R., Seelig, J., Eds; Springer-Verlag: Berlin, 1991; Vol. 23, p 165.

(34) Forsyth, D. A.; Sebag, A. B. *J. Am. Chem. Soc.* **1997**, *119*, 9483−9494.

(35) Desiraju, G. R. *Chem. Commun.* **2005**, 2995−3001.

(36) Nishio, M. *CrystEngComm* **2004**, *6*, 130−158.

(37) Arunima; Kurur, N. D. *Chem. Phys. Lett.* **2005**, *401*, 470−474.

(38) Pena Ruiz, T.; Fernández-Gómez, M.; López González, J. J.; Koziol, A. E.; Granadino Roldán, J. M. *J. Mol. Struct.* **2004**, *707*, 33−46.

(39) Rahman, A. N. M. M.; Bishop, R.; Craig, C. D.; Scudder, M. L. *Eur. J. Org. Chem.* **2003**, 72−81.

(40) Ciunik, Z.; Desiraju, G. R. *Chem. Commun.* **2001**, 703−704.

TABLE 3. Correlation between Experimental (DMSO-d_6) and Theoretical ^{13}C Chemical Shift Values for Compounds 1a−e,[a] Together with the Quadratic Sum of All Deviations[b] and the Relative Population Calculated for α and *β* Tautomers[c]

	1a		1b		1c		1d		1e	
	α	*β*	α	*β*	α	*β*	α	*β*	α	*β*
R^2	0.9932	0.9856	0.9596	0.9481	0.9973	0.9913	0.9984	0.9906	0.9971	0.9866
$\Sigma\Delta\delta^2$	68.5	128.7	420.5	469.9	110.0	192.1	359.8	861.6	339.6	491.2
pop%	65.3	34.7	52.8	47.2	63.6	36.4	70.5	29.5	59.1	40.9

[a] All numerical values are available as Supporting Information. [b] Deviations $\Delta\delta\%$ are evaluated as $\Delta\delta\% = 100(\delta_{calcd} - \delta_{expt})/\delta_{expt}$; $\Sigma\Delta\delta^2$ is the quadratic sum of all deviations $\Delta\delta\%$. [c] Calculated as $pop\%_{\alpha\beta} = 100[\Sigma\Delta\delta_{\beta\alpha}{}^2/(\Sigma\Delta\delta_{\alpha}{}^2 + \Sigma\Delta\delta_{\beta}{}^2)]$.

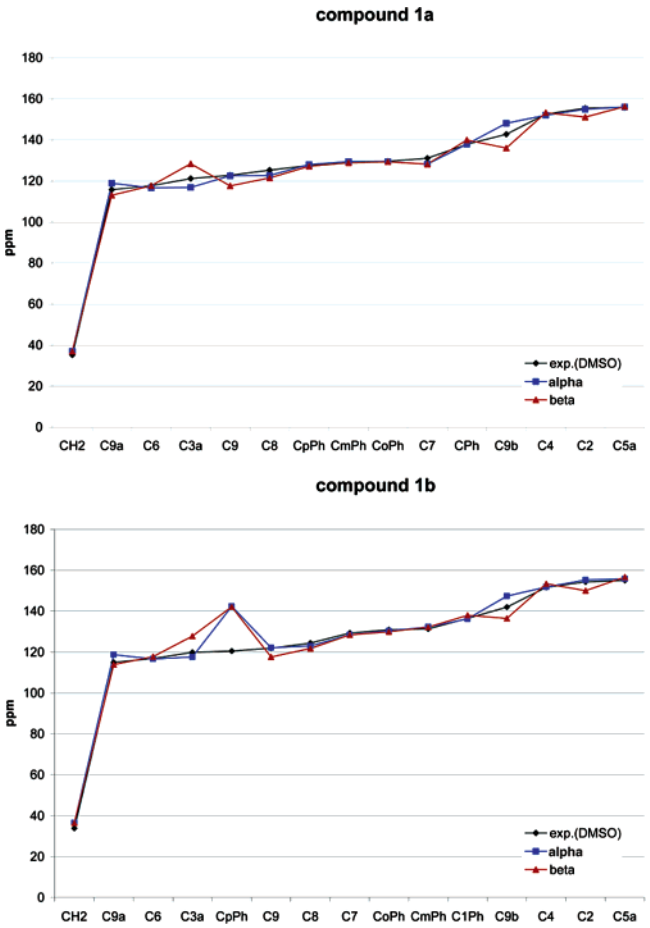

FIGURE 3. Experimental vs theoretical ^{13}C chemical shifts for compounds **1a** and **1b**.

3). It should be noted that $\Sigma\Delta\delta^2$ values calculated for compounds **1b**, **1d**, and **1e** were quite high, evidencing some discrepancy between computed and experimental values. For compounds **1d** and **1e**, this fact was easy to explain by the presence of three carbon atoms lying in the low-frequency region, where a lower accuracy in terms of $\Delta\delta\%$ was expected due to the major percent weight of systematic errors. For compound **1b**, instead, the source of the error was the presence of a bromine-substituted carbon, as a consistent spin−orbit effect is detectable for heavy halogen-substituted carbons and such effect induces a notable overestimation of the computed ^{13}C chemical shift, as shown in Figure 3.[43] However, the above-mentioned errors were of the same magnitude for both tautomers, and thus they were not relevant for the study of the tautomeric equilibrium investigated here. Results reported in Table 3 showed that the tautomeric equilibrium was shifted toward the α form for all the investigated compounds, in accordance with enthalpy calculation results.

Percent populations reported in Table 3 did not follow the same trend observed before, showing an α tautomer population of about 70% for compound **1d** and 53% for compound **1b**. Compounds **1a**, **1c**, and **1e** lay in the middle with percent values of 65, 64, and 59%, respectively. A further comparison with experimental results was then desirable to determine which of the above-described theoretical methods provided the most accurate description of the tautomeric equilibria investigated here.

Dynamic ^{1}H NMR and Coalescence Temperature Measurements. At room temperature the ^{1}H NMR spectra, recorded in d_6-acetone, for compounds **1a**−**e** showed a broad singlet at about 12−13 ppm, corresponding to the N−H, and a broad signal at about 8 ppm corresponding to the coumarin C9−H. ^{1}H NMR spectra were then recorded for compounds **1a**−**e** by systematically lowering the probe temperature until the maximum separation $\Delta\nu$ was observed between split signals or until the solubility limit was reached. To exclude any dependence between concentration and tautomeric equilibrium, it has to be noted that ^{1}H spectra were recorded at different sample concentrations and no relevant differences were observed. The initial splitting of the C9−H signal, together with the broadening of the N−H, was observed between 269 K (**1a**) and 197 K (**1c**). Low-temperature spectra were characterized by two singlet signals for the N−H and two doublets for C9−H lying at 13−13.5 ppm and 7.9−8.1, respectively. Within the couple of N−H and C9−H signals, intensity differences showed the presence of a major and a minor tautomer. As usual, the N−H signals of the less abundant tautomer were broader than those belonging to the major tautomer.[17] It should be reported that the unequivocal assignment of such signals to tautomer α or *β* was attempted through several NOESY and ROESY experiments, although room-temperature experiments did not provide the expected results due to the fast chemical exchange observed between the α and *β* tautomers. Moreover, low temperatures were not reachable as compounds **1a**−**e** crystallized in the NMR probe due to their low solubility limits combined with the long acquisition time requested, although it was quite clear that a correct assignment of ^{1}H signals to each tautomeric form could reasonably be made on the basis of the comparison of free energy and ^{13}C calculations and available experimental results. However, even the most accurate theoretical prediction should not be treated as an experimental certainty, and for this reason, describing dynamic NMR results, we referred to major and minor instead of α and *β* tautomer. As depicted in Figures 4−6, lower temperatures caused a significant shift of the N−H signal to higher frequencies, whereas they affected the position of the C9−H and aromatic signals in a decidedly minor way. This is not surprising as mobile hydrogens are strongly affected by the experimental conditions. The coumarin aromatic proton regions were particularly interesting and will be hereafter described for compound **1d** where the lack of the aromatic substituent made

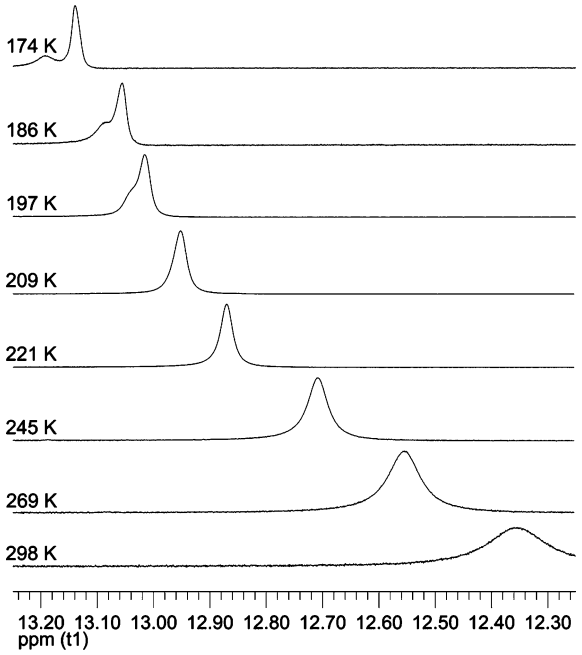

FIGURE 4. Coalescence of the N−H signals of **1d**.

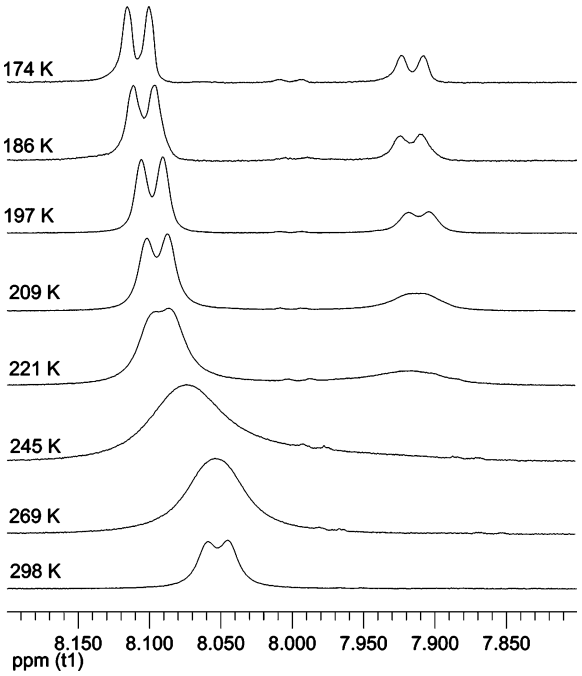

FIGURE 5. Coalescence of the C9−H signals of **1d**.

the interpretation of all the coumarin proton signals easier. As depicted in Figure 6, at room temperature an overlapped double double doublet and a broad doublet were detected at 7.55 and 7.44 ppm, respectively. Those signals did not split with decreasing temperature and could reasonably be assigned to protons C7−H and C6−H, respectively. Indeed, at room temperature, where the resolution was quite good, we measured two J_{ortho} of 8.4 and 8.5 Hz and a J_{meta} of 1.5 Hz within the former signal, and a J_{ortho} of 8.5 Hz was measured in the latter. The J_{meta} was not measurable due to low resolution. Finally, a pseudo triplet was observable at 7.41 ppm, and this signal split with decreasing temperature in the most and least intense signals at 7.49 and 7.44 ppm, respectively. Unfortunately, such a signal

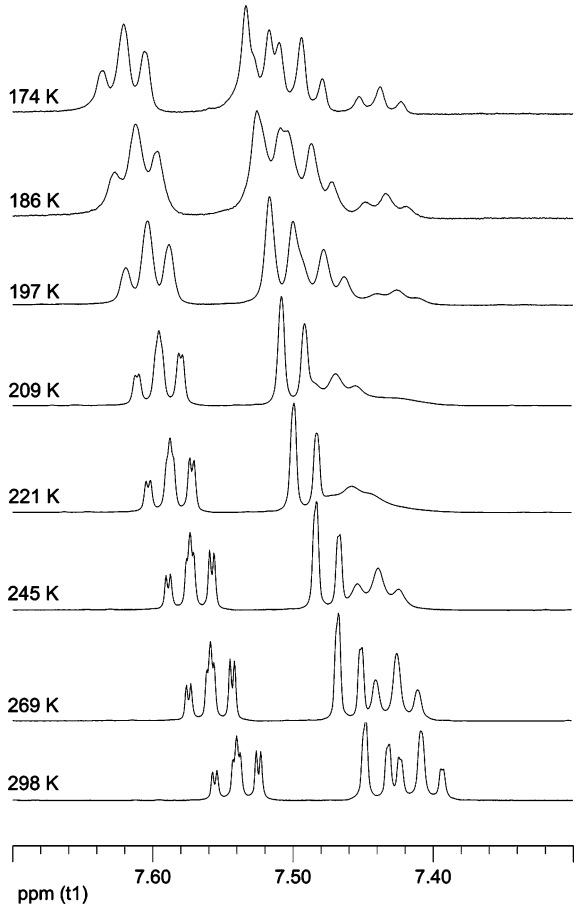

FIGURE 6. Coalescence in the aromatic proton region of **1d**.

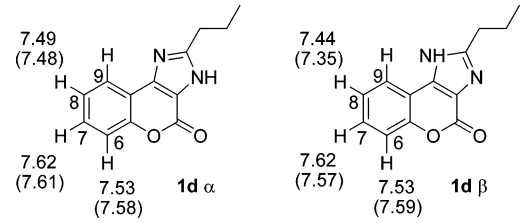

FIGURE 7. ^{1}H chemical shifts for C8−H, C7−H and C6−H registered at 174 K, theoretical B3LYP/TZVP values in parentheses.

was not resolved enough for an accurate coupling constants measurement, probably due to the dynamic character of the signal itself, although such a signal could be assigned only to the C8−H proton, and the observed splitting showed that also the C8−H proton is strongly influenced by the tautomeric process. As depicted in Figure 7, theoretically calculated ^{1}H chemical shifts supported our interpretation of the aromatic proton region.

Finally, but not surprisingly, split signals were also observable at low temperatures for the aliphatic hydrogens of the side chain: at room temperature, the CH_2 protons of compounds **1a**,**b** were characterized by a singlet at 4.34 and 4.33 ppm, respectively, while at low temperature, a major and a minor singlet were observable at 4.33 and 4.25 ppm for **1a** and at 4.32 and 4.23 ppm for **1b**. An analogue behavior was observed for both **1d** and **1e**. At low temperature, the former compound showed two split signals corresponding to the methyl linked and to the C2 linked CH_2 (1.83 and 2.91 ppm, respectively, for the major tautomer, 1.77 and 2.83 ppm for the minor), while

TABLE 4. ^{1}H Chemical Shifts for C9−H, α−β Percent Population, Coalescence Temperature Measurements, and Corresponding α−β Tautomerization Barrier for Compounds 1a−e[a]

	δ (ppm)		pop%[b]				
compd	major	minor	major	minor	$\Delta\nu$[c] (Hz)	T_s[d] (K)	T_c[e] (K)
1a	8.09	7.85	67.6	32.4	116.1	209	269
1b	8.08	7.88	58.5	41.5	99.8	174	209
1c	8.12	7.90	68.5	31.5	112.7	174	197
1d	8.11	7.92	69.4	30.6	99.1	174	245
1e	8.12	7.93	63.7	36.3	91.6	174	206

[a] ^{1}H NMR spectra were registered in acetone-d_6. Signal C9−H was chosen for percent population measurements. [b] Populations of the major and minor tautomer, evaluated from signal C9−H integrals at temperature T_s. [c] Maximum observed separation between the coalescent proton signals at T_s. [d] Temperature at which the maximum separation $\Delta\nu$ is observed. [e] Coalescence temperature.

the CH_3 signal did not split. Compound **1e** showed split signals for the *i*-pr CH_3 (1.32 and 1.38 ppm for the minor and major tautomers, respectively) and for the *i*-pr C−H (3.21 and 3.29 for the minor and major tautomers, respectively). Surprisingly, compound **1c** did not show split signals relative to the ethylphenyl side chain, but for the signal at 3.25 ppm we observed only a line broadening together with loss of resolution.

As reported in Table 4, the C9−H signals did not show relevant differences in chemical shift among compounds **1a**−**e**, assuming values between 8.08 (compound **1b**) and 8.12 ppm (compounds **1c** and **1e**) for the most intense signal, while the least intense one fell between 7.85 (compound **1a**) and 7.93 ppm (compound **1e**). Percent populations of each tautomer were measured by integrating the respective C9−H signals on spectra recorded at the temperature providing the highest $\Delta\nu$ between the major and the minor signal. Consequently, the major tautomer population resulted within 58.5 and 69.4% as obtained for compounds **1b** and **1d**, respectively. Compounds **1a** and **1c** provided values close to the upper limit (67.6 and 68.5%, respectively), while compound **1e** lay in the middle with a population of 63.7%. Percent populations reported in Table 4 were in particularly good accordance with the values obtained from the comparison of theoretical and experimental ^{13}C chemical shifts (see Table 3), confirming this latter method as the most predictive for the study of tautomeric equilibrium.

Whenever a chemical exchange is observable through NMR experiments, coalescence temperature measurements can be used to estimate the energetic barrier associated with the process.[42,44] This technique was successfully applied for the study of conformational mobility[45−47] as well as for the prediction of tautomerization barriers for nitrogen containing heterocycles.[47,48] Concerning compounds investigated here, the coalescence of the C9−H signal was observable within a temperature between 200 and 270 K, corresponding to a tautomerization barrier of 9−13 kcal/mol as evaluated from standard equations.[49,50] Such results were quite concordant with tautomerization barriers measured in solution for different azoles, which are in the range of 10−14 kcal/mol as reported in the literature.[51−54] Interestingly, as one can see from Table 4, the coalescence temperatures and related $\Delta G^{\ddagger}$ values were not dependent on the chemical features of the C2 linked substituent, such as steric hindrance, branching of the side chain, or the presence of an aromatic ring. Similarly, we did not observe any dependency between coalescence temperature and tautomer percent populations, and for the above-mentioned reasons the different tautomeric behavior observed within compounds **1a**−**e** remained unclear. Indeed, compounds **1a** and **1d** showed the highest coalescence temperature, resulting in $\Delta G^{\ddagger}$ values of 12.6 and 11.6 kcal/mol, respectively. On the contrary, the lowest $\Delta G^{\ddagger}$ was calculated for compound **1c** (9.2 kcal/mol), while compounds **1b** and **1e** showed quite similar tautomerization barriers of 9.8 and 9.7 kcal/mol, respectively.

Conclusions

The thorough study of the tautomerism of 2-substituted benzopyranoimidazolones in solution was possible through a combination of theoretical and experimental techniques, where one method filled in the gaps of the other. We could reasonably affirm that the only tautomeric equilibrium observable in solution was between the N3−H and N1−H forms, namely the α and β tautomers, respectively, and that the α tautomer was the most abundant. Energy calculations were accurate enough to estimate the position of the tautomeric equilibrium, but the comparison of theoretical and experimental ^{13}C chemical shifts provided more accurate results. We could then conclude that gas-phase B3LYP/TZVP//B3LYP/6-31G** resulted in an adequate method for the calculation of ^{13}C chemical shifts finalized to the study of tautomerism, as it provided quite high accuracy at a reasonable computational cost. Through dynamic ^{1}H NMR experiments, we demonstrated that not only N−H and C9−H but also C8−H and side-chain protons were highly influenced by tautomerism.

Experimental Section

General Methods. Compounds **1a**−**e** are known compounds, and they were prepared according to procedures described in the literature.[3]

NMR Measurements. Dynamic ^{1}H NMR were recorded in d_6-acetone in a temperature range from 298 to 173 K on a 500 MHz

(41) Optimization was allowed for all variables, except the constrained N1−C2−C1′−C2 (for **1a**,**d**) and N1−C2−C1′−H (for **1e**) dihedrals.

(42) Bain, A. D. *Prog. Nucl. Magn. Reson. Spectrosc.* **2003**, *43*, 63−103.

(43) Kaupp, M.; Malkina, O. L.; Malkin, V. G.; Pyykkö, P. *Chem.−Eur. J.* **1998**, *4*, 118−126.

(44) Abraham R. J.; Loftus, P. In *Proton and Carbon-13 NMR Spectroscopy: An Integrated Approach*; Heyden and Sons: London, 1980; Chapter 5 and section 7.4 of Chapter 7.

(45) Gasparro F. P.; Kolodny, N. H. *J. Chem. Educ.* **1977**, *54*, 258−261.

(46) Lam P. C.-H.; Charlier, P. R. *J. Org. Chem.* **2005**, *70*, 1530−1538.

(47) Dall'Oglio, E.; Caro, M. B.; Gesser, J. C.; Zucco, C.; Rezende, M. C. *J. Braz. Chem. Soc.* **2002**, *13*, 251−259.

(48) Dolenský, B.; Kroulík, J.; Král, V.; Sessler, J. L.; Dvořáková, H.; Bouř, P.; Bernátková, M.; Bucher, C.; Lynch, V. *J. Am. Chem. Soc.* **2004**, *126*, 13714−13722.

(49) From the Eyring equation $k_c = \pi/2^{1/2}\Delta\nu = RT_c/Nh \exp(-\Delta G^{\ddagger}/RT_c)$, where T_c is the coalescence temperature in Kelvin, k_c is the exchange rate constant at T_c, $\Delta\nu$ is the maximum separation in hertz observed between the two coalescing proton signals, N is Avogadro's number, and h is Planck's constant. Therefore, after numerical solution, $\Delta G^{\ddagger} = 4.54 \times 10^{-3}\, T_c(9.97 + \log T_c - \log \Delta\nu)$ kcal/mol.

(50) Denk, M. K. *CHEM 2070 Structure and Spectroscopy − NMR Spectroscopy*. University of Guelph. http://131.104.156.23/Lectures/CHEM_207/CHM_207_NMR.htm, summer 2005.

(51) Roumestant, M. L.; Viallefont, P.; Elguero, J.; Jacquier, R. *Tetrahedron Lett.* **1969**, 495−498.

(52) Chenon, M. T.; Coupry, C.; Grant, D. M.; Pugmire, R. J. *J. Org. Chem.* **1977**, *42*, 695−661.

(53) Claramunt, R. M.; Elguero, J.; Marzin C.; Seita, J. *Anal. Quim.* **1979**, *75*, 701−706.

(54) Perrin, M.; Thozet, A.; Cabildo, P.; Claramunt, R. M.; Valenti, E.; Elguero, J. *Can. J. Chem.* **1993**, *71*, 1443−1449.

spectrometer with a recently calibrated temperature control unit. The coalescence temperature was determined to the nearest 10 K.

Theoretical Calculations. All ab initio and DFT calculations were performed using either the Gaussian 98[21] or the Gaussian 03 package.[22] Starting geometries were initially obtained through a conformational search at the AM1 level.[23] The most stable conformers were completely optimized in a vacuum at the B3LYP/6-31G** level,[24,25] and frequencies were calculated at the same level to confirm the minimized structures as a minimum (no imaginary frequencies). To investigate any dependency between relative enthalpies and temperature, the thermochemical analysis was repeated at 298, 273, 253, 233, 213, and 193 K, and no relevant ΔH differences between tautomers were observed within this temperature range. The solvation effect was studied using both the PCM[26] and CPCM[27] model for DMSO and acetone; however, CPCM was more robust and provided better accordance with the available experimental results. Vacuum and solution energies were evaluated by single-point calculations at the B3LYP/TZVP level.[28] NMR computations were performed on the most stable conformers as evaluated at the B3LYP/TZVP//B3LYP/6-31G** level both in the gas phase and in solution. The absolute shieldings of all tautomers were calculated using the GIAO method.[29,30] To choose a reliable theoretical level to describe our specific problem, preliminary computations were performed on the $N-CH_3$ derivative **2d**, as for such a compound the tautomerization is not allowed. Absolute shieldings σ were computed on the B3LYP/6-31G** optimized geometries at the HF and B3LYP levels using the 6-31G**, 6-311+G(2d,p), TZVP, and cc-pVTZ basis sets.[31] The solvent effect on the determination of chemical shifts was evaluated at the HF/6-311+G(2d,p) and B3LYP/TZVP levels using the PCM and CPCM models. The correlation coefficient R^2 between the theoretical and experimental values was used to choose the best computational method for our purpose. Regarding ^{13}C NMR, gas-phase B3LYP/TZVP and B3LYP/cc-pVTZ calculations provided a really good fit with experiments, showing both linear correlation with $R^2 = 0.9992$. However, the former method was a better performer in terms of CPU time. The inclusion of the solvent effect by both the PCM and CPCM models in NMR computation did not afford appreciable improvement ($R^2 = 0.9992$ for PCM, $R^2 = 0.9993$ for CPCM, evaluated at the B3LYP/TZVP level on the test compound **2d**) but notably increased the computation time, as it was also observed by other authors.[32] For the above-mentioned reasons all theoretical chemical shifts reported in this work were calculated in gas phase at the B3LYP/TZVP//B3LYP/6-31G** level. To obtain better comparison between theoretical and experimental data, ^{13}C σ values computed by the GIAO method were converted in chemical shifts δ by a regression analysis. This method was successfully adopted by several authors as it avoids the subtraction of a standard reference (i.e., TMS) from the computed absolute shieldings, thus reducing the possibility to introduce systematic errors in calculated δ.[33,34] Therefore, linear regression analysis was performed by the comparison of the experimental δ values with the computed σ values for compound **2d**, where tautomerism is suppressed by N-methylation, leading to the equation:

$$\delta^{13}\mathrm{C(ppm)} = (176.226 \pm 0.748) - (0.968 \pm 0.0808)\sigma\mathrm{(ppm)} \quad (1)$$

where $n = 14$ and $R^2 = 0.999$. Equation 1 was then applied for the calculation of ^{13}C chemical shifts for compounds **1a**−**e**.

Acknowledgment. We thank the MIUR for financial support, the CILEA for computational facilities, and Dr. Giorgio Abbiati for the critical examination of the manuscript and for useful conversations.

Supporting Information Available: Atomic coordinates and energies of α, β, γ, and δ tautomers of compounds **1a**−**e**; relative energies from the potential energy surface scan for the rotation of the C2−C1′ σ-bond for compounds **1a**,**d**,**e**; theoretical and experimental ^{13}C chemical shifts with percent deviations; experimental ^{1}H chemical shifts (d_6-acetone) for compounds **1a**−**e**. This material is available free of charge via the Internet at http://pubs.acs.org.

JO0519256